DOI: 10.1002/ejic.201000664

Synthesis, Crystal Structures, and Luminescent Properties of Noninterpenetrating (6,3) Type Network Lanthanide Metal–Organic Frameworks Assembled by a New Semirigid Bridging Ligand

Qin Wang,[a] Kuan-Zhen Tang,[a] Wei-Sheng Liu,[a] Yu Tang,*[a] and Min-Yu Tan[a]

Keywords: Lanthanides / Metal–organic frameworks / Semirigid bridging ligands / Homometallic compounds / Luminescence

A series of lanthanide metal–organic frameworks (MOFs) possessing 4f homometallic 2D noninterpenetrating (6,3) honeycomb topological network structures with lanthanide atoms acting as three-connected centers have been assembled by using a semirigid bridging ligand with lanthanide nitrates, namely $[\{Ln_2(NO_3)_6L_3\}\cdot(H_2O)_2\cdot(CHCl_3)]_n$ (Ln = Pr, Nd, Sm, Eu, Gd, Tb, Dy, Er; L = 2,5-dimethyl-1,4-bis[{(2′-benzylaminoformyl)phenoxy}methyl]benzene. The coordination layers are linked by intermolecular hydrogen bonds to form a 3D cage structure with 1D supramolecular channels along the *c* axis, in which chloroform and lattice water molecules are located to stabilize the structure. Under specific excitation, the Sm^{III}, Eu^{III}, Tb^{III}, and Dy^{III} MOFs exhibit characteristic emissions. The lowest triplet-state energy level of the ligand indicates that the energy level of the ligand matches better to the resonance levels of Tb^{III} and Dy^{III} rather than Sm^{III} and Eu^{III} ions.

Introduction

The use of metal ions to control the self-assembly of composite metal–organic frameworks (MOFs) represents a burgeoning field that may offer functional solid materials as well as fascinating molecular structures.[1] In particular, the purposeful construction of molecular aggregates, such as grid, porous, helix, rotaxane, catenane, and knot structures,[2] are based on crystal engineering principles and the coordination geometry of metal ions. This means that the reasoned selection of ligands can lead to the assembly of MOFs with a variety of structures and topologies. Until now much attention has been paid to transition metal MOFs,[3] whereas lanthanide homometallic MOFs have received less consideration.[4] Recently, lanthanide MOFs have attracted more interest because of their interesting structural diversity[5] and special properties such as porosity,[6,7] nonlinear optics,[8] luminescence,[9] and magnetism,[10] as well as an intriguing variety of architectures and molecular topologies.[11] Thus, it is becoming increasingly evident that despite continuous endeavours to understand the molecular structure and topology of MOFs with lanthanide centers, the control and prediction of lanthanide coordination networks are still a great challenge because of the high coordination number and flexible coordination geometry of lanthanide ions and structural characteristics of polydentate organic ligands.[12] Recently, a variety of new lanthanide MOFs have been constructed by the careful design of ligands. For example, rigid polyfunctional ligands are well known to form rods, grids, bricks, honeycombs, and diamondoid nets,[13] whereas flexible linear ligands may facilitate formation of helicates and other intertwined supermolecules.[14] Rigid polyfunctional ligands have the advantage of forming ordered open networks defined by metal coordination geometries but also frequently suffer from the phenomenon of interpenetration and supramolecular isomerization.[15] Lanthanide MOFs and semirigid ligands are important objects for investigation because of their potential as luminescent sensors and building blocks for flexible MOFs, respectively. Therefore, the assembly of lanthanide MOFs by using semirigid ligands will be a very interesting attempt to construct microporous materials. Herein we designed and prepared a new semirigid bridging ligand incorporating an aromatic skeleton bearing two salicylamide arms, 2,5-dimethyl-1,4-bis[{(2′-benzylaminoformyl)phenoxy}methyl]benzene (L), which may provide a fascinating means to assembling unusual lanthanide MOFs possessing excellent luminescent properties, as salicylamide-derived ligands are generally efficient sensitizers of lanthanide luminescence.[16] As a result, a series of new lanthanide MOFs, $[\{Ln_2(NO_3)_6L_3\}\cdot(H_2O)_2\cdot(CHCl_3)_6]_n$ [Ln = Pr (**1**), Nd (**2**), Sm (**3**), Eu (**4**), Gd (**5**), Tb (**6**), Dy (**7**), and Er (**8**)], were

[a] Key Laboratory of Nonferrous Metal Chemistry and Resources Utilization of Gansu Province, State Key Laboratory of Applied Organic Chemistry, College of Chemistry and Chemical Engineering, Lanzhou University, Lanzhou 730000, P. R. China
Fax: +86-931-8912582
E-mail: tangyu@lzu.edu.cn

Supporting information for this article is available on the WWW under http://dx.doi.org/10.1002/ejic.201000664.

assembled by the reaction between the ligand and the lanthanide nitrates. Structural analyses of the complexes **3**, **4**, **6**, and **8** reveal that the complexes possess 4f homometallic 2D noninterpenetrating (6,3) honeycomb topological networks with 1D supramolecular channels along the *c* axis located by the positions of chloroform and lattice water molecules. To date, only a few reports are concerned with the diversity of (6,3) honeycomb-based structures controlled by homometallic Ln ions.[4b–4d] The luminescent properties of the MOFs formed with Ln^{3+} [Ln = Sm (**3**), Eu (**4**), Tb (**6**), and Dy (**7**)] were also studied in detail.

Results and Discussion

Characterization of the Complexes

Elemental analysis and molar conductivity data (Table S1) indicate that the eight complexes have a 2:3:6 metal/ligand/nitrate stoichiometry. The molar conductance (Λ_m [$S\,cm^2\,mol^{-1}$]) of the complexes in methanol solutions indicate that all complexes act as nonelectrolytes,[17] implying that the nitrate groups are in the coordination sphere.

The characteristic bands in the IR spectra of the complexes are similar (Table S2). The IR spectrum of the free ligand shows bands at 1644 and 1228 cm^{-1}, which are assigned to ν(C=O) and ν(Ar–O–C), respectively. In the complexes, the low-energy band remains unchanged, but the high-energy band redshifts to about 1628–1610 cm^{-1}, indicating that only the oxygen atom of the C=O group takes part in coordination to the metal ion. The characteristic frequencies of the coordinating nitrate groups (C_{2v}) appear at 1483–1508 (ν_1), 1286–1298 (ν_4), 1029–1032 (ν_2), and 813–817 (ν_5) cm^{-1}. The difference between the two strongest absorptions (ν_1 and ν_4) of the nitrate groups is 189–213 cm^{-1}, and the absence of bands at 1380, 820, and 720 cm^{-1} in the spectra of the complexes indicates that no free nitrate groups (D_{3h}) are present. This clearly establishes that all the NO_3^- groups in the solid complexes coordinate to the lanthanide ion as bidentate ligands.[18] The broad bands at ca. 3400 cm^{-1} are ascribed to water molecules in the complexes.

Crystal Structures of the Lanthanide MOFs 3, 4, 6, and 8

Single-crystal X-ray analyses reveal that the isomorphous complexes with Sm (**3**), Eu (**4**), Tb (**6**), and Er (**8**) all crystallize in the trigonal space group $P\bar{3}$, displaying a 2D honeycomb framework in the *ab* plane, which can be regarded as a (6,3) topological network with the lanthanide atoms acting as three-connected centers. Herein we describe **4** in detail. In complex **4**, the ligands act as bridging linkers through the carbonyl oxygen atoms. The asymmetric unit of **4** contains a third each of an Eu atom and an NO_3^- anion and half of a ligand. Figure 1a shows the coordination sphere around each Eu^{3+} center, which consists of six oxygen atoms coming from three bidentate nitrate groups (O3, O4) and three oxygen atoms coming from three salicylamide arms of three separate ligands (O1). The coordination environment of the nine-coordinate Eu^{3+} center is a distorted tricapped trigonal prism (Figure 1b). The Eu–O(nitrate) bond lengths span the range 2.506(3)–2.511(3) Å, and the Eu–O(carbonyl) bond lengths are 2.335(3) Å, which are comparable to the corresponding Eu–O bond lengths found in related complexes.[4d] Each ligand acts as an *exo*-bidentate linker and binds to two Eu^{3+} centers using the two carbonyl oxygen atoms of the amide groups. Thus, each ligand is coordinated to two Eu^{3+} ions, and each Eu^{3+} ion is coordinated to three ligands to form a 3:2 (L/M) complex. Six ligand linkers alternately bridge six $Eu(NO_3)_3$ moieties to form a hexagonal 102-membered ring, in which three nonadjacent europium atoms are coplanar, paralleling the remaining three nonadjacent europium atoms with a plane-to-plane distance of 13.985 Å. The hexagonal rings are edge-sharing to each other, yielding a 2D honeycomb framework in the *ab* plane (Figure 1c), which can be regarded as a (6,3) topological network with europium atoms acting as three-connected nodes and $Eu(L)_{3/2}(NO_3)_3$ units as repeating units. None of the counterions, NO_3^-, lie in cavities within the network but bind to the Eu^{3+} centers. This makes the framework a completely neutral network. In this case, the (6,3) net is not the ubiquitous flat graphene sheet but a topologically equivalent (6,3) net of chair-conformation six-membered rings, which form a coordination polymer analogue of the puckered layers in graphite monofluoride, CF_x.[19] The layers of **4** stack together parallel to the *c* axis, and noninterpenetration of networks is observed, which should be avoided in order to construct molecular microporous materials. Furthermore, the corrugated honeycomb layers are stacked in an AAA manner along the *c* axis to produce a 3D hexagonal channel (Figure 1d). The assembly of a honeycomb structure is challenging since the hexagon represents the most common pattern in nature and is familiar from benzene to the honeycomb of the bee. It is uncommon to generate honeycomb networks by using semirigid amide ligands and, to the best of our knowledge, this type of noninterpenetrating neutral lanthanide homometallic (6,3) topological frameworks with large macrometallocycles constructed with semirigid amide ligands is few. In addition, the coordination layers are linked by intermolecular hydrogen bonds O···H–N (listed in Table 1) to form a 3D cage supermolecule. Moreover, 1D channels along the *c* axis are formed and are occupied by the chloroform and lattice water molecules, which make the framework more stable (Figure 2). The internal dimensions of the channels have been evaluated to be about 4.9% of the structure (total potential solvent volume of 184.7 $Å^3$ per unit cell volume of 3781.4 $Å^3$) calculated with PLATON.[20] This compares with 32% (total potential solvent volume of 1211.4 $Å^3$ out of per-unit cell volume of 3781.4 $Å^3$) if chloroform and lattice water molecules are omitted.

To further investigate the thermal behaviors of these MOFs, thermogravimetric analysis (TGA) of **6** was carried out in air from 25 to 800 °C. The weight loss of lattice water

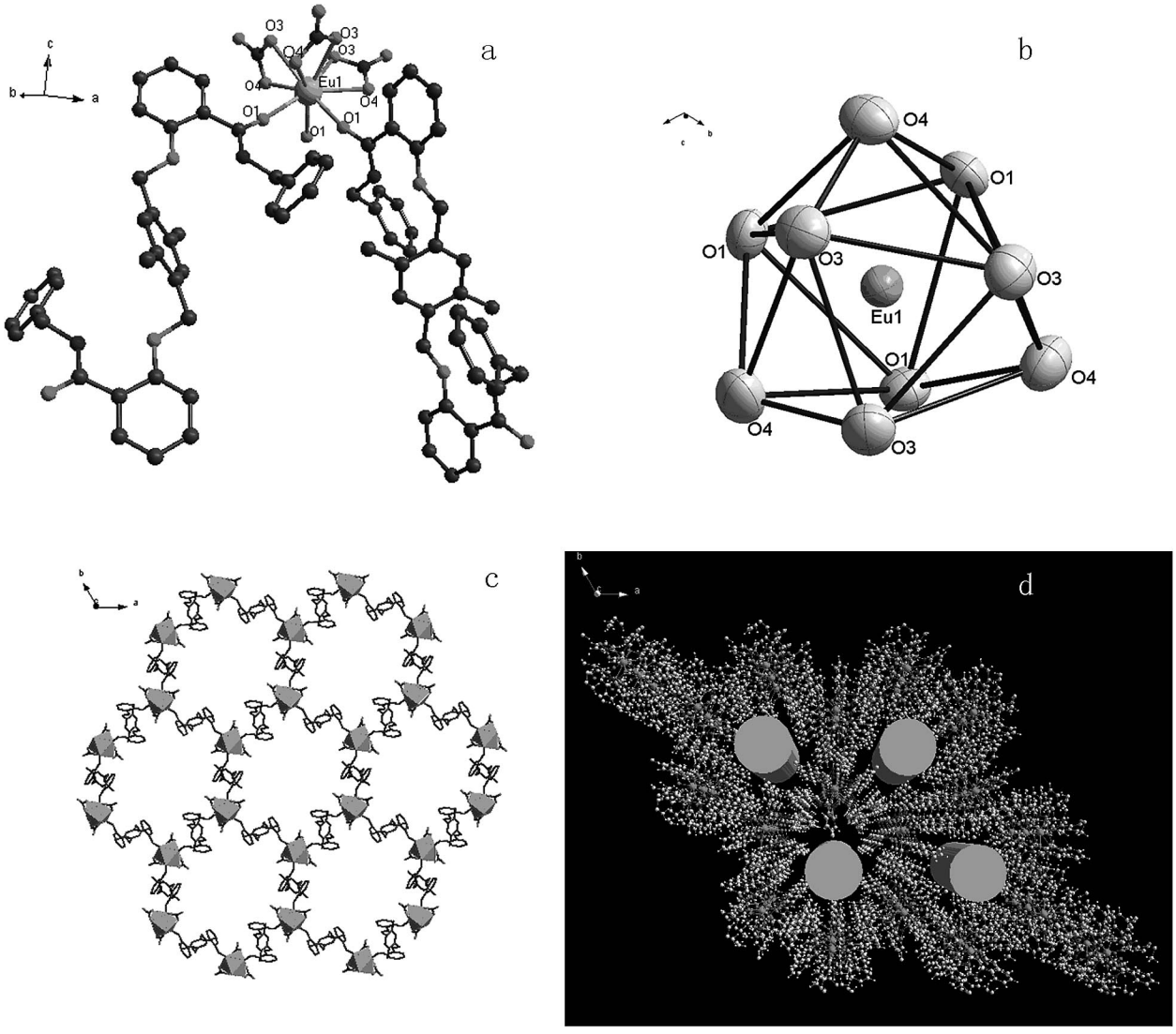

Figure 1. (a) Structure of **4** showing the coordination sphere of Eu^{3+} along with atom labeling schemes, (b) coordination polyhedron of Eu, (c) view of the 2D honeycomb (6,3) topology network of the complex in the *ab* plane (the benzyl groups of the ligands, hydrogen atoms, and chloroform and water molecules are omitted for clarity), and (d) view of 3D noninterpenetrating honeycomb layers of (6,3) topology with 1D channels along the *c* axis showing the 1D perforative column-like channels (hydrogen atoms, crystallized chloroform, and lattice water molecules are omitted for clarity).

and chloroform molecules occurs at 81, 133, 215, and 243 °C (calculated: 23.57%; observed: 22.43%). The host framework remains stable up to 446 °C and then collapses rapidly. The residue that remains is Tb_4O_7. The total weight loss of 87.37% is in accordance with the calculated value of 88.29%. XRD analysis showed obvious changes after the removal of the solvents (Figure S1), proving the stabilizing effect of the solvents on the structure of the MOFs.

What greatly impresses us is that these complexes show 2D noninterpenetrating (6,3) honeycomb structures where the bis(salicylamide) ligands take part in coordination with the metal ions, whereas previously described lanthanide complexes with analogous ligands conform zig zag chains or rings connected by chain 1D coordination polymers.[21] We have deduced that the skeleton, the confinement of the terminal groups of the ligands, and the conformational distortions of the ligands[4d] can all affect the molecular structure of the complexes.

The crystal structures of the four complexes indicate that the coordination environments of the metal ions are protected by three separate ligands and three bidentate nitrate groups. Since coordinated solvent molecules, especially water, can efficiently quench lanthanide luminescence, the ability to satisfy the coordination requirements of the lanthanide(III) centre with a high coordination number and reinforce the stability of the MOFs without additional bound solvent molecules plays an important role in the design of luminescent MOFs.

Table 1. Hydrogen-bond lengths [Å] and angles [°] of complexes **3**, **4**, **6**, and **8**.

Complex	D–H···A	*d*(D–H)	*d*(H···A)	*d*(D···A)	∠DHA	
3	N(2)–H(2)···O(5)	0.86	1.96	2.624(9)	133	
	C(3)–H(3)···O(3)	0.93	2.43	2.753(11)	100	
	C(3)–H(3)···O(2)	0.93	2.50	3.420(10)	171	1 – *y*, 1 + *x* – *y*, *z*
	C(8)–H(8A)···O(3)	0.97	2.43	2.806(8)	103	
	C(8)–H(8A)···O(3)	0.97	2.54	3.491(10)	166	–*x* + *y*, 1 – *x*, *z*
	C(8)–H(8B)···O(1 W)	0.97	2.59	3.502(18)	156	
	C(15)–H(15B)···O(1)	0.97	2.58	3.521(11)	162	1 – *x*, 1 – *y*, –*z*
	C(20)–H(20)···O(4)	0.98	2.42	3.24(2)	142	*y*, –*x* + *y*, –*z*
4	N(1)–H(1A)···O(2)	0.86	1.95	2.613(5)	133	
	C(7)–H(7A)···O(1)	0.97	2.42	2.800(6)	103	
	C(7)–H(7A)···O(1)	0.97	2.52	3.471(7)	167	1 – *y*, 1 + *x* – *y*, *z*
	C(7)–H(7B)···O(1 W)	0.97	2.59	3.504(13)	157	
	C(10)–H(10)···O(3)	0.93	2.49	3.408(7)	171	
	C(15)–H(15B)···O(4)	0.97	2.58	3.512(8)	161	*y*, –*x* + *y*, 1 – *z*
6	N(1)–H(1A)···O(2)	0.86	1.95	2.615(6)	133	
	C(7)–H(7A)···O(1)	0.97	2.44	2.811(6)	102	
	C(7)–H(7A)···O(1)	0.97	2.51	3.455(7)	166	–*x* + *y*, 1 – *x*, *z*
	C(7)–H(7B)···O(6 W)	0.97	2.58	3.486(14)	156	
	C(10)–H(10)···O(3)	0.93	2.46	3.385(7)	172	1 – *y*, 1 + *x* – *y*, *z*
	C(15)–H(15B)···O(4)	0.97	2.60	3.540(7)	163	1 – *x*, 1 – *y*, –*z*
	C(20)–H(20)···O(5)	0.98	2.53	3.30(3)	136	*y*, –*x* + *y*, –*z*
8	N(2)–H(2A)···O(7)	0.86	1.95	2.615(11)	133	
	C(7)–H(7A)···O(8)	0.97	2.44	2.809(8)	102	
	C(7)–H(7A)···O(8)	0.97	2.46	3.418(10)	168	1 – *y*, 1 + *x* –*y*,*z*
	C(7)–H(7B)···O(4)	0.97	2.59	3.503(15)	157	
	C(14)–H(14)···O(1)	0.93	2.43	3.357(11)	174	–*x* + *y*, 1 – *x*, *z*
	C(20)–H(20)···O(3)	0.98	2.54	3.28(2)	132	*y*, –*x* + *y*, 1 – *z*

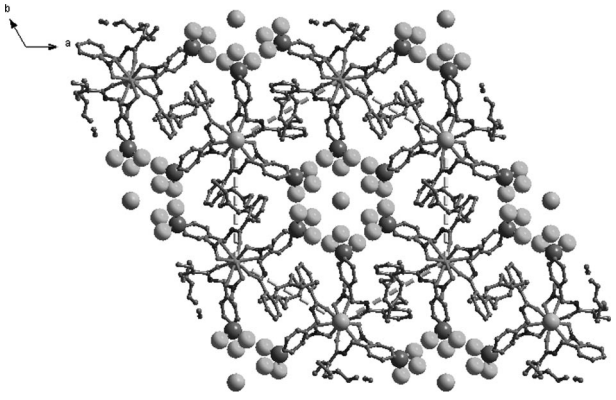

Figure 2. Chloroform and lattice water molecules in 1D channels of **4**.

Electronic Spectra

The electronic spectra in the visible region of the Ln^{III} complexes exhibit alternations in intensity and shifts in position of the absorption bands relative to the corresponding Ln^{III}–aquo ions. Jørgensen has attributed this shift to the effect of the interelectronic repulsion between the 4f electrons on the crystal field, and is related to the covalent character of the metal–ligand bond, assessed by Sinha's parameter (δ), the nephelauxetic ratio (β), and the bonding parameter ($b^{1/2}$).[22]

Absorption spectra of **1**, **2**, and **8** were recorded in methanol solutions at room temperature, and the covalence parameters were calculated (Table 2). The values of β, which are less than unity, and positive values of δ and $b^{1/2}$ for **2** indicate that the metal–ligand bonds have some covalent character.[23] The β value for **8** is more than unity and the δ value is negative, suggesting that the Er^{3+}–O bond has a less covalent character than that of the Er^{3+}–aquo ion.

Table 2. Electronic spectroscopic data and covalence parameters of **1**, **2** and **8**. The frequencies in parentheses are the electronic spectroscopic data for the corresponding Ln^{III}–aquo ions.

Complex	Frequency [cm^{-1}]	Assignment	Covalence parameters
1	16592 (16595)	$^3H_4 \rightarrow {}^1D_2$	β = 0.9982
	20704 (21085)	$^3H_4 \rightarrow {}^3P_1$	δ = 0.1803
	21267 (21255)	$^3H_4 \rightarrow {}^1I_6$	$b^{1/2}$ = 0.0640
	22522 (22290)	$^3H_4 \rightarrow {}^3P_2$	
2	12563 (12608)	$^4I_{9/2} \rightarrow {}^2H_{9/2}$	β = 0.9985
	13550 (13435)	$^4I_{9/2} \rightarrow {}^4S_{3/2}$	δ = 0.1502
	17271 (17203)	$^4I_{9/2} \rightarrow {}^2G_{7/2}$	$b^{1/2}$ = 0.0274
	19120 (19414)	$^4I_{9/2} \rightarrow {}^4G_{9/2}$	
8	15384 (15136)	$^4I_{15/2} \rightarrow {}^4F_{9/2}$	β = 1.0098
	19230 (19147)	$^4I_{15/2} \rightarrow {}^2H_{11/2}$	δ = –0.9705
	20491 (20313)	$^4I_{15/2} \rightarrow {}^4F_{7/2}$	

Luminescent Properties of Complexes in the Solid State

Upon UV irradiation, the free ligands emit a strong blue luminescence (apparent λ_{max} at 446 nm). However, upon complexation, this emission is replaced by the corresponding lanthanide cation emitting in the visible range (Sm^{3+}, Eu^{3+}, Tb^{3+}, and Dy^{3+}), which can be readily seen with the naked eye, indicating the occurrence of ligand-to-metal in-

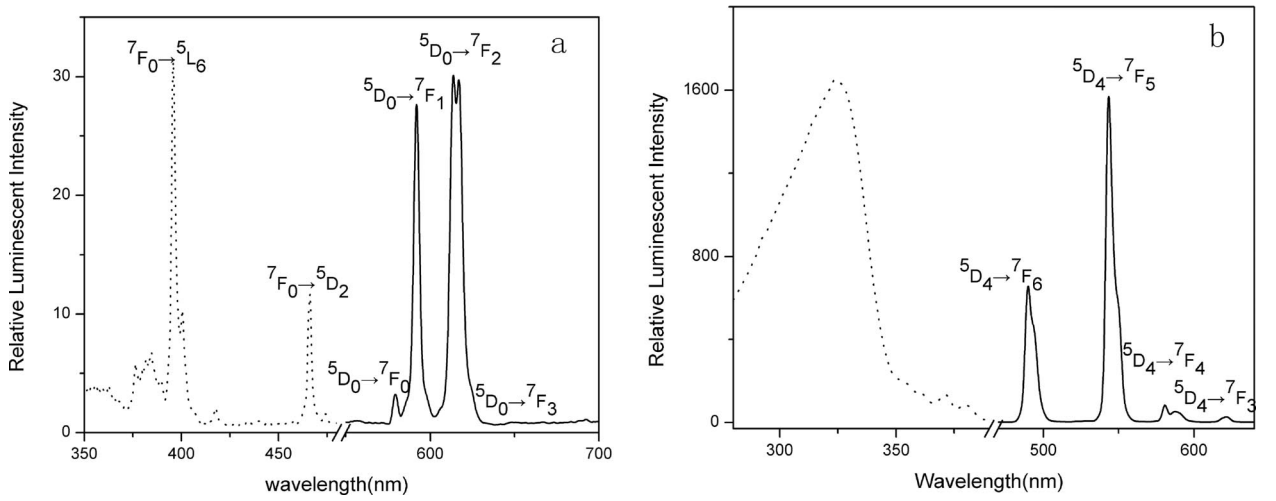

Figure 3. Room-temperature excitation and emission spectra of (a) **4** and (b) **6** in the solid state (EX slit = 1.0 nm, EM slit = 2.5 nm).

tramolecular photoinduced energy transfer. To examine the ability of the ligands to be antenna groups for sensitized luminescence from lanthanides, we compared the luminescent properties of **4** and **6**.

The solid-state excitation and emission spectra of **4** and **6** at room temperature are shown in Figure 3, and the relevant photophysical data are summarized in Table 3. The excitation spectrum of **4** has negligible contribution from the ligand and exhibits a series of sharp lines characteristic of the Eu^{3+} energy-level structure.[24] This indicates that luminescence sensitization of **4** through excitation of the ligand is not efficient. The emission peaks of **4** at 580, 592, 614, 617, and 694 nm can be assigned to $^5D_0\rightarrow{}^7F_J$ (J = 0, 1, 2, 4) transitions of the Eu^{III} ion. Notably, the intensity of the $^5D_0\rightarrow{}^7F_2$ transition (electric dipole) is slightly stronger than that of the $^5D_0\rightarrow{}^7F_1$ transition (magnetic dipole), indicating the absence of an inversion center at the Eu^{III} site, which is in agreement with the single-crystal X-ray analysis.[25] The fluoroscence quantum yield (Φ) of the Eu^{III} complex in the solid state was found to be 1.03% by using an integrating sphere. The luminescence decay of **4** is best described by a single-exponential process with a lifetime (τ) of 1.291 ± 0.001 ms.

The excitation spectrum of **6** revealed the characteristic emission of a Tb^{3+} ion in the solid state (Figure 3b), which overlaps the absorption spectrum in the 280–380 nm region. This indicates a very efficient energy transfer from the ligand to the central Tb^{3+} ion. The room-temperature normalized emission spectrum of **6** exhibits characteristic emission bands for Tb^{3+} centred at 490, 543, 581, and 621 nm, which result from relaxation of the $^5D_4$ excited state to the corresponding ground state ^7F_J (J = 6, 5, 4, 3) of the Tb^{3+} ion. The most intense emission is centred at 543 nm and corresponds to the hypersensitive $^5D_4\rightarrow{}^7F_5$ transition. The ligand fluorescence disappears completely, indicating a very efficient energy transfer from the ligand to the central Tb^{3+} ion. Furthermore, compared to the as-prepared sample, the luminescence intensity increased clearly after removal of the solvents. This could be attributed to the elimination of the lattice water molecules in **6**, which quench the luminescence of the central Tb^{III} ion. In the solid state **6** has a value of 31.13% for Φ by using an integrating sphere at room temperature. The solid-state luminescence lifetime value for the $^5D_4$ level of **6** was determined to be 2.124 ± 0.001 ms from the luminescence decay profile at room temperature by fitting with a monoexponential curve.

Table 3. Photophysical characterization for the complexes **3**, **4**, **6**, and **7**, where RLI is the relative luminescent intensity.

Complex	λ_{max}[a] [nm]	RLI [au]	τ[b] [ms]	Φ[b] [%]
3	563.4	2.396		0.81
	597.4	2.424		
4	579.4	3.321	1.291±0.001	1.03
	591.8	28.14		
	613.6	30.80		
	617.0	30.46		
	648.4	0.845		
	692.6	1.105		
6	489.8	668.6	2.124±0.001	31.13
	543.4	1592		
	580.6	84.35		
	621.4	25.78		
7	482.2	116.2		5.60
	573.0	88.84		

[a] EX slit = 1.0 nm, EM slit = 2.5 nm. [b] Luminescence lifetimes and quantum yields are reported here with an error of ±15%.

The potential for the antenna-modified ligand (L) to sensitize other visible-light-emitting lanthanide cations, notably Sm^{3+} and Dy^{3+}, was also evaluated. For complex **3**, two characteristic bands can be observed, which are attributed to $^4G_{5/2}\rightarrow{}^6H_J$ (J = 5/2, 7/2) transitions (Figure 4a). For complex **7**, two characteristic narrow bands can be seen in the emission spectrum, which are attributed to transitions of $^4F_{9/2}\rightarrow{}^6H_{15/2}$ (482 nm) and $^4F_{9/2}\rightarrow{}^6H_{13/2}$ (573 nm) (Figure 4b). Quantum-yield measurements for **3** and **7** in the solid state were found to be 0.81% and 5.60%, respectively. The fluorescence quantum yields of the four complexes

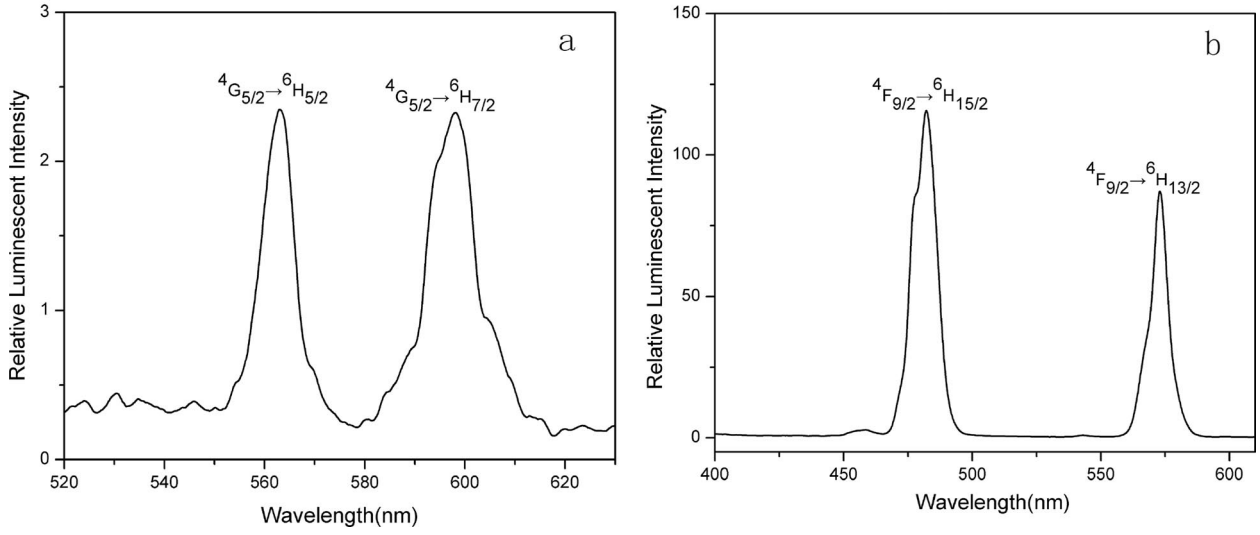

Figure 4. Room-temperature emission spectra of (a) **3** and (b) **7** in the solid state excited at 325 nm (EX slit = 1.0 nm, EM slit = 2.5 nm).

(Table 3) follow the trend **6** > **7** > **4** > **3**, which means that the energy transfer from the organic ligands to Tb^{III} and Dy^{III} is more effective than that to Eu^{III} and Sm^{III}. This behaviour can be rationalized by the ligand-to-metal energy transfer discussed below.

Energy Transfer between the Ligand and Ln^{III}

An intramolecular energy transfer from the triplet state of the ligand to the resonance level of the Ln^{III} ion is one of the most important processes that has an influence on the Ln^{III} luminescent properties of Ln^{III} chelates.[26] A triplet excited state, T_1, is localized on one ligand only and is independent of the nature of the lanthanide ion. In order to acquire T_1 of the ligand, the phosphorescence spectrum of **5** was measured at 77 K (Figure S2) in a methanol/ethanol mixture (v/v = 1:1). From the phosphorescence spectra, T_1 of **5**, which corresponds to the lower wavelength emission edge,[27] is 24390 cm^{-1} (410 nm). Because the lowest excited state, $^6P_{7/2}$ (32000 cm^{-1}) of Gd^{III} is much higher than the lowest-lying triplet levels of most chromophores, the data obtained from the phosphorescence spectrum actually reveals the triplet energy level of the ligand in the complex. Latva's empirical rule[28] states that an optimal ligand-to-metal energy transfer process for Ln^{III} needs [$\Delta E = E(T_1) - E(^5D_J)$] 2500–4500 cm^{-1} for Tb^{III} and 2500–4000 cm^{-1} for Eu^{III}. The experimentally observed T_1 energy level of the ligand is ca. 3890 cm^{-1} higher than the $^5D_4$ level of Tb^{III} (20500 cm^{-1}) and ca. 3390 cm^{-1} higher than the $^4F_{9/2}$ level of Dy^{III} (21000 cm^{-1}), which facilitates efficient energy transfer. By contrast, the lowest energy Eu^{III} and Sm^{III} acceptor levels are at 17300 ($^5D_0$) and 17900 cm^{-1} ($^4G_{5/2}$), respectively, which are significantly lower in energy than the T_1 energy level of the ligand. This supports the observation of stronger sensitization of **6** and **7** than **3** and **4** because of the larger energy gap between the ligand triplet and the Sm^{III} and Eu^{III} excited states.

Conclusions

We have presented a new amide semirigid bridging ligand forming noninterpenetrating (6,3) type cage MOFs with lanthanide cations through the carbonyl oxygen donors. We deduce that there may be two reasons for the interesting result. Firstly, the semirigid bis(monodentate) nature of the ligand makes it easy to bind to two Ln^{III} ions by using the two oxygen atoms of the amide groups. This is one of the key factors in the construction of the backbone of the 2D MOFs. Nitrate was selected as a suitable counterion to replace the water molecules in the coordination sphere of the Ln ion. The additional three bidentate nitrates satisfy the need of a high coordination number, and they can also improve the luminescence and stability of MOFs. Ligands containing salicylamide terminal groups exhibit a good antenna effect for Ln^{3+} cations and provide excellent sensitization of Tb^{3+} luminescence through a particularly efficient ligand-to-lanthanide energy transfer process. To sum up, we have designed a new semirigid bridging ligand with two long arms, which can strongly bind Ln^{3+} ions to form elegant lanthanide MOFs and sensitize Tb^{3+} luminescence emission. The coupling of MOFs and luminescence in a material has interesting prospects for the development of lanthanide-based luminescent materials.

Experimental Section

Synthesis and Characterizations: Lanthanide nitrates,[29] *N*-benzylsalicylamide,[30] and 1,4-bis(bromomethyl)-2,5-dimethylbenzene[31] were prepared according to literature methods. Other chemicals were obtained from commercial sources and used without purification.

Preparation and Characterization of the Ligand: The synthetic route for the preparation of the ligand is shown in Scheme S1. *N*-Benzylsalicylamide (3.39 g, 15.0 mmol), anhydrous potassium carbonate (2.07 g, 15.0 mmol), and acetone (50 mL) were warmed to ca. 90 °C before 1,4-bis(bromomethyl)-2,5-dimethylbenzene (1.46 g,

5.0 mmol) was added. The reaction mixture was heated to reflux with stirring for 8 h. After cooling, the mixture was filtered, and the resulting solid was washed with water and acetone to obtain the ligand. Yield 85%, m.p.162–164 °C, ^{1}H NMR ($CDCl_3$, 300 MHz): δ = 2.12 (s, 6 H), 4.49–4.50 (d, 4 H), 5.08 (s, 4 H), 7.05–7.25 (m, 16 H), 7.45–7.50 (t, 2 H), 8.13 (s, 2 H), 8.28–8.30 (d, 2 H) ppm.

Preparation and Characterization of the Complexes: A solution of the ligand (0.15 mmol L) in chloroform (10 mL) was added dropwise to a solution of $Ln(NO_3)_3{\cdot}6H_2O$ (Ln = Pr, Nd, Sm, Eu, Gd, Tb, Dy, Er) (0.1 mmol L) in ethyl acetate (10 mL). The mixture was stirred at room temperature for 4 h before the precipitated solid complex was collected by filtration, washed with ethyl acetate/chloroform (v/v = 1:1) and dried in vacuo over P_4O_{10} for 48 h. Yield: 80%. All of the complexes are diffluent in DMF and DMSO, soluble in methanol and acetone, slightly soluble in ethanol, acetonitrile, and ethyl acetate, and have low solublility in chloroform, diethyl ether, and petroleum ether. Single crystals of **3**, **4**, **6**, and **8** were grown from acetone/chloroform (v/v = 1:1) solutions with slow concentration at room temperature for ca. 3 weeks.

Physical Measurements: C, H, N elemental analyses were carried out with an Elementar Vario EL. IR spectra were recorded in the 4000–400 cm^{-1} region from KBr pellets with a Nicolet Nexus 670 FT-IR spectrometer. ^{1}H NMR spectra were measured with a Varian Mercury 300 spectrometer in $CDCl_3$ solutions with TMS as an internal standard. Electronic spectra were recorded with a Varian Cary 100 spectrophotometer in methanol solutions. Luminescence spectra and phosphorescence spectra were obtained with a Hitachi F-4500 fluorescence spectrophotometer. The quantum yields of **6** and **7** were determined by an absolute method with an integrating sphere (150 mm diameter, $BaSO_4$ coating) from Edinburgh Instruments FLS920. The lifetime measurement was measured with an Edinburgh Instruments FLS920 Fluorescence Spectrometer with an Nd-pumped OPOlette laser as the excitation source. TG analysis was performed with a Perkin–Elmer thermal analyzer up to 800 °C at a heating rate of 10 °C/min under static air. X-ray diffraction patterns were determined with a Rigaku-Dmax 2400 diffractometer using Cu-K_α radiation.

X-ray Crystallographic Analyses of the Complexes: The X-ray diffraction data were collected with graphite-monochromated Mo-K_α radiation with a Bruker CCD area detector diffractometer and were collected with the ω-2θ scan technique. The crystal structures were solved by direct methods. All non-hydrogen atoms were refined anisotropically by full-matrix least-squares methods on F^2. Primary non-hydrogen atoms were solved by direct methods and secondary non-hydrogen atoms were solved by difference maps. The hydrogen atoms were added geometrically and not refined. All calculations were performed by using the programs SHELXS-97 and SHELXL-97.[32,33] The crystal data and refinement results are summarized in Table S1. Selected bond lengths and angles are given in Table S2. CCDC-614821 (**3**), -614820 (**4**), -614822 (**6**), and -614819 (**8**) contain the supplementary crystallographic data for this paper. These data can be obtained free of charge from The Cambridge Crystallographic Data Center (CCDC) via www.ccdc.cam.ac.uk/data_request/cif.

Supporting Information (see footnote on the first page of this article): Elemental analyses and molar conductivity data, IR spectra, crystallography data, selected bond lengths and angles, phosphorescence spectrum of **5** at 77 K, and the synthetic route for the ligand.

Acknowledgments

This work was supported by the National Natural Science Foundation of China (Projects 20931003, 20401008) and the Program for New Century Excellent Talents in University (NCET-06-0902).

[1] a) G. B. Gardner, D. Venkataraman, J. S. Moore, S. Lee, *Nature* **1995**, *374*, 792–795; b) O. M. Yaghi, G. Li, H. Li, *Nature* **1995**, *378*, 703–706; c) C.-Y. Duan, M.-L. Wei, D. Guo, C. He, Q.-J. Meng, *J. Am. Chem. Soc.* **2010**, *132*, 3321–3330; d) Z.-F. Tian, J.-G. Lin, Y. Su, L.-L. Wen, Y.-M. Liu, H.-Z. Zhu, Q.-J. Meng, *Cryst. Growth Des.* **2007**, *7*, 1863–1867; e) Q. Yue, Q. Sun, A.-L. Cheng, E.-Q. Gao, *Cryst. Growth Des.* **2010**, *10*, 44–47; f) A. J. Blake, N. R. Champness, P. Hubberstey, W. S. Li, M. A. Withersby, M. Schröder, *Coord. Chem. Rev.* **1999**, *183*, 117–138.

[2] a) M. Fujita, *Acc. Chem. Res.* **1999**, *32*, 53–61; b) D.-G. Ding, B.-L. Wu, Y.-T. Fan, H.-W. Hou, *Cryst. Growth Des.* **2009**, *9*, 508–516; c) D. Hagrman, C. Zubieta, D. J. Rose, J. Zubieta, R. C. Haushalter, *Angew. Chem. Int. Ed. Engl.* **1997**, *36*, 873–876; d) X.-Q. Liang, D.-P. Li, X.-H. Zhou, Y. Sui, Y.-Z. Li, J.-L. Zuo, X.-Z. You, *Cryst. Growth Des.* **2009**, *9*, 4872–4883.

[3] a) C. Janiak, *Angew. Chem. Int. Ed. Engl.* **1997**, *36*, 1431–1434; b) O. R. Evans, R. G. Xiong, Z. Wang, G. K. Wong, W. Lin, *Angew. Chem. Int. Ed.* **1999**, *38*, 536–538; c) X.-L. Zhang, C.-P. Guo, Q.-Y. Yang, T.-B. Lu, Y.-X. Tong, C.-Y. Su, *Chem. Mater.* **2007**, *19*, 4630–4632; d) Y. J. Kim, Y. J. Park, D. Y. Jung, *Dalton Trans.* **2005**, 2603–2609; e) J.-L. C. Rowsell, E. C. Spencer, J. Eckert, J.-A. K. Howard, O. M. Yaghi, *Science* **2005**, *309*, 1350–1354; f) F.-Q. Wang, X.-J. Zheng, Y.-H. Wan, C.-Y. Sun, Z.-M. Wang, K.-Z. Wang, L.-P. Jin, *Inorg. Chem.* **2007**, *46*, 2956–2958; g) R. Murugavel, D. Krishnamurthy, M. Sathiyendiran, *J. Chem. Soc., Dalton Trans.* **2002**, 34–39; h) M. Xue, G.-S. Zhu, Y.-J. Zhang, Q.-R. Fang, I. J. Hewitt, S.-L. Qiu, *Cryst. Growth Des.* **2008**, *8*, 427–434; i) C. C. Stoumpos, R. Inglis, G. Karotsis, L. F. Jones, A. Collins, S. Parsons, C. J. Milios, G. S. Papaefstathiou, E. K. Brechin, *Cryst. Growth Des.* **2009**, *9*, 24–27.

[4] a) J.-G. Wang, C.-C. Huang, X.-H. Huang, D.-S. Liu, *Cryst. Growth Des.* **2008**, *8*, 795–798; b) X. Li, Y.-B. Zhang, M. Shi, P.-Z. Li, *Inorg. Chem. Commun.* **2008**, *11*, 869–872; c) Q. Wang, K.-Z. Tang, W.-S. Liu, Y. Tang, M.-Y. Tan, *J. Solid State Chem.* **2009**, *182*, 3118–3124; d) Y.-L. Guo, W. Dou, X.-Y. Zhou, W.-S. Liu, W.-W. Qin, Z.-P. Zang, J.-R. Zhang, D.-Q. Wang, *Inorg. Chem.* **2009**, *48*, 3581–3590; e) Y.-Z. Zhang, J.-R. Li, S. Gao, H.-Z. Kou, H.-L. Sun, Z.-M. Wang, *Inorg. Chem. Commun.* **2002**, *5*, 28–31; f) C. Kremer, J. Torres, S. Domínguez, *J. Mol. Struct.* **2008**, *879*, 130–149.

[5] A. Heba, J. B. Graham, J. J. Lu, M. Brian, R. P. Ian, B. W. Rosa, J. Z. Michael, *Cryst. Growth Des.* **2003**, *3*, 513–519.

[6] Z. Ni, A. Yassar, T. Antoun, O. M. Yaghi, *J. Am. Chem. Soc.* **2005**, *127*, 12752–12753.

[7] J.-L. C. Rowsell, O. M. Yaghi, *Angew. Chem. Int. Ed.* **2005**, *44*, 4670–4679.

[8] T.-F. Liu, J. Lü, Z.-G. Guo, D. M. Proserpio, R. Cao, *Cryst. Growth Des.* **2010**, *10*, 1489–1491.

[9] a) B. D. Chandler, D. T. Cramb, G.-K. H. Shimizu, *J. Am. Chem. Soc.* **2006**, *128*, 10403–10412; b) B.-L. Chen, L.-B. Wang, F. Zapata, G.-D. Qian, E.-B. Lobkovsky, *J. Am. Chem. Soc.* **2008**, *130*, 6718–6719; c) P. I. Girginova, F. A. Almeida Paz, P.-C. R. Soares-Santos, R. A. Sá Ferreira, L. D. Carlos, V. S. Amaral, J. Klinowski, H.-I. S. Nogueira, T. Trindade, *Eur. J. Inorg. Chem.* **2007**, 4238–4246.

[10] a) E. Coronado, J. R. Galan-Mascaros, C. J. Gomez-Garcia, V. Laukhin, *Nature* **2000**, *408*, 447–449; b) M. Andruh, J.-P. Costes, C. Diaz, S. Gao, *Inorg. Chem.* **2009**, *48*, 3342–3359.

[11] S. R. Batten, R. Robson, *Angew. Chem. Int. Ed.* **1998**, *37*, 1460–1494.

[12] a) X.-P. Yang, C.-Y. Su, B.-S. Kang, X.-L. Feng, W.-L. Xiao, H.-Q. Liu, *J. Chem. Soc., Dalton Trans.* **2000**, 3253–3260; b) X.-P. Yang, B.-S. Kang, W.-K. Wong, C.-Y. Su, H.-Q. Liu, *Inorg. Chem.* **2003**, *42*, 169–179; c) R. Sun, S.-N. Wang, H. Xing, J.-F. Bai, Y.-Z. Li, Y. Pan, X.-Z. You, *Inorg. Chem.* **2007**, *46*, 8451–8453; d) W.-S. Liu, T.-Q. Jiao, Y. Li, Q. Liu, M.-Y. Tan, H. Wang, L.-F. Wang, *J. Am. Chem. Soc.* **2004**, *126*, 2280–2281; e) H.-L. Gao, L. Yi, B. Zhao, X.-Q. Zhao, P. Cheng, D.-Z. Liao, S.-P. Yan, *Inorg. Chem.* **2006**, *45*, 5980–5988.

[13] a) A. J. Blake, N. R. Champness, P. Hubberstey, W.-S. Li, M. A. Withersby, M. Schröder, *Coord. Chem. Rev.* **1999**, *183*, 117–138; b) L. Carlucci, G. Ciani, P. Macchi, D. M. Proserpio, *Chem. Commun.* **1998**, 1837–1838; c) B. F. Abrahams, J. Coleiro, B. F. Hoskins, R. Robson, *Chem. Commun.* **1996**, 603–604; d) O. M. Yaghi, H. Li, *J. Am. Chem. Soc.* **1996**, *118*, 295–296; e) K. A. Hirsch, D. Venkataraman, S. R. Wison, J. S. Moor, S. Lee, *J. Chem. Soc., Chem. Commun.* **1995**, 2199–2200; f) H.-P. Wu, C. Janiak, G. Rheinwald, H. Lang, *J. Chem. Soc., Dalton Trans.* **1999**, 183–190.

[14] a) M. Fujita, F. Ibukuro, H. Seki, O. Kamo, M. Imanari, K. Ogura, *J. Am. Chem. Soc.* **1996**, *118*, 899–900; b) D. B. Amabilino, C. O. Dietrich-Buchecker, J.-P. Sauvage, *J. Am. Chem. Soc.* **1996**, *118*, 3285–3286; c) D. Whang, K. Kim, *J. Am. Chem. Soc.* **1997**, *119*, 451–452; d) D. P. Funeriu, J.-M. Lehn, K. M. Fromm, D. Fenske, *Chem. Eur. J.* **2000**, *6*, 2103–2111.

[15] a) M. J. Zaworotko, *Angew. Chem. Int. Ed.* **1998**, *37*, 1211–1213; b) S. R. Batten, R. Robson, *Angew. Chem. Int. Ed.* **1998**, *37*, 1461–1494.

[16] a) J. Zhang, Y. Tang, N. Tang, M.-Y. Tan, W.-S. Liu, K.-B. Yu, *J. Chem. Soc., Dalton Trans.* **2002**, 832–833; b) Y. Tang, J. Zhang, W.-S. Liu, M.-Y. Tan, K.-B. Yu, *Polyhedron* **2005**, *24*, 1160–1166; c) X.-Q. Song, W. Dou, W.-S. Liu, Y.-L. Guo, X.-L. Tang, *Inorg. Chem. Commun.* **2007**, *10*, 1058–1062; d) X.-Q. Song, W.-S. Liu, W. Dou, Y.-W. Wang, J.-R. Zheng, Z.-P. Zang, *Eur. J. Inorg. Chem.* **2008**, 1901–1912.

[17] W. J. Geary, *Coord. Chem. Rev.* **1971**, *7*, 81–122.

[18] a) N. F. Curtis, Y. M. Curtis, *Inorg. Chem.* **1965**, *4*, 804–808; b) A.-B. P. Lever, E. Mantovani, B. S. Ramaswamy, *Can. J. Chem.* **1971**, *49*, 1957–1964.

[19] a) T. J. Prior, M. J. Rosseinsky, *Chem. Commun.* **2001**, 495–496; b) Y.-L. Wang, D.-Q. Yuan, W.-H. Bi, X. Li, X.-J. Li, F. Li, R. Cao, *Cryst. Growth Des.* **2005**, *5*, 1849–1855.

[20] A. L. Spek, *PLATON, A Multipurpose Crystallographic Tool*, Utrecht University, Utrecht, The Netherlands, **2003**.

[21] a) C.-L. Yi, Y. Tang, W.-S. Liu, M.-Y. Tan, *Inorg. Chem. Commun.* **2007**, *10*, 1505–1509; b) D.-Y. Liu, Z.-Q. Kou, Y.-F. Li, K.-Z. Tang, Y. Tang, W.-S. Liu, M.-Y. Tan, *Inorg. Chem. Commun.* **2009**, *12*, 461–464.

[22] a) C. K. Jørgenson, *Prog. Inorg. Chem.* **1962**, *4*, 73–124; b) S. P. Sinha, *Spectrochim. Acta* **1966**, *22*, 57–62; c) D. E. Henrie, G. R. Choppin, *J. Chem. Phys.* **1968**, *49*, 477–481.

[23] a) A. K. Solanki, A. M. Bhandaka, *J. Inorg. Nucl. Chem.* **1979**, *41*, 1311–1314; b) S.-X. Liu, W.-S. Liu, X.-L. Wang, M.-Y. Tan, *Polyhedron* **1995**, *14*, 3605–3609.

[24] a) R. Shyni, S. Biju, M.-L. P. Reddy, A. H. Cowley, M. Findlater, *Inorg. Chem.* **2007**, *46*, 11025–11030; b) S. Biju, D.-B. A. Raj, M.-L. P. Reddy, B. M. Kariuki, *Inorg. Chem.* **2006**, *45*, 10651–10660.

[25] A. F. Kirby, D. Foster, F. S. Richardson, *Chem. Phys. Lett.* **1983**, *95*, 507–512.

[26] M. Latva, H. Takalo, V. M. Mukkala, C. Matachescu, J. C. Rodriguez-Ubis, J. Kankare, *J. Lumin.* **1997**, *75*, 149–169.

[27] W. Dawson, J. Kropp, M. Windsor, *J. Chem. Phys.* **1966**, *45*, 2410–2418.

[28] N. Arnaud, J. Georges, *Spectrochim. Acta Part A* **2003**, *59*, 1829–1840.

[29] K. Nakagawa, K. Amita, H. Mizuno, Y. Inoue, T. Hakushi, *Bull. Chem. Soc. Jpn.* **1987**, *60*, 2037–2040.

[30] K. Michio, *Bull. Chem. Soc. Jpn.* **1976**, *49*, 2679–2682.

[31] M. R. Dahrouch, P. Jara, L. Mendez, Y. Portilla, D. Abril, G. Alfonso, I. Chavez, J. M. Manriquez, M. Riviēre-Baudet, P. Riviēre, A. Castel, J. Rouzaud, H. Gornitzka, *Organometallics* **2001**, *20*, 5591–5597.

[32] G. M. Sheldrick, *Acta Crystallogr., Sect. A* **1990**, *46*, 467–473.

[33] G. M. Sheldrick, *SHELXS-97, A Program for X-ray Crystal Structure Solution*, and *SHELXL-97, A Program for X-ray Structure Refinement*, Göttingen University, Germany, **1997**.

Received: June 17, 2010
Published Online: October 11, 2010

